agronomy

MDPI

Article

Time-Course Transcriptome and Phytohormonal Analysis of Blue-Light-Induced Adventitious Root Development of Tea Cuttings (*Camellia sinensis* (L.) Kuntze)

Yaozong Shen [1,2,†], Hui Wang [3,†], Xiao Han [2], Kai Fan [2], Jiazhi Shen [1], He Li [2], Shibo Ding [3], Dapeng Song [3], Yu Wang [2,*] and Zhaotang Ding [1,*]

[1] Tea Research Institute, Shandong Academy of Agricultural Sciences, Jinan 250100, China
[2] Tea Research Institute, Qingdao Agricultural University, Qingdao 266109, China
[3] Tea Research Institute, Rizhao Academy of Agricultural Sciences, Rizhao 276800, China
* Correspondence: wangyutea@163.com (Y.W.); dzttea@163.com (Z.D.)
† These authors contributed equally to this work.

Abstract: *C. sinensis* is an economically important crop for tea production that experiences increasing demand and good export potential. Therefore, crops need to be expanded, and high-quality planting material is required. Vegetative propagation by cuttings is the prevalent method; therefore, this paper explored its optimization potential modeled on cultivar 'Jiukengzao'. This study wanted to deeply explore blue-light-induced adventitious root formation and development of tea cuttings, so we conducted short-term (0 h, 8 h, and 16 h) and long-term (30 d, 60 d, and 90 d) time-course analyses on tea cutting seedlings. Short-term, full-length transcriptome analysis showed that the expression of genes related to plant hormone signal transduction and auxin transport was highest at 16 h. Sixteen hours of light was considered as suitable for adventitious root growth and development of tea cuttings. Long-term phytohormone analysis showed that the trend of indole-3-carboxylic acid (ICA) change was: 60 d > 90 d > 30 d. Long-term, full-length transcriptome analysis showed that the gene expression trends in K2, K5, K6, and K8 clusters were: 90 d > 60 d > 30 d, and the opposite was observed in K1, K4, and K11 clusters. Kyoto Encyclopedia of Genes and Genomes (KEGG) analysis showed that most of the genes in these seven clusters are involved in "plant hormone signal transduction (ko04075)". This includes auxin early responsive protein *AUX/IAA*, auxin response factor *ARF*, auxin-responsive protein *SAUR*, etc. In addition, genes related to auxin transport and synthesis were identified as *PIN1*, *3*, *4*, *PILS2*, *6*, *7*, flavin-containing monooxygenase *YUC9*, and *YUC10*, and the expression trend of these genes was mostly consistent with the change trend of ICA content. This study further explained the molecular mechanism of blue-light-induced adventitious root formation and development of tea cuttings. It is recommended that blue light can be used to promote the adventitious root growth and development of tea cuttings in practical production.

Keywords: tea cutting; blue light; time-course analysis; full-length transcriptome; k-means; phytohormone

Citation: Shen, Y.; Wang, H.; Han, X.; Fan, K.; Shen, J.; Li, H.; Ding, S.; Song, D.; Wang, Y.; Ding, Z. Time-Course Transcriptome and Phytohormonal Analysis of Blue-Light-Induced Adventitious Root Development of Tea Cuttings (*Camellia sinensis* (L.) Kuntze). *Agronomy* **2023**, *13*, 1561. https://doi.org/10.3390/agronomy13061561

Academic Editor: Youssef Rouphael

Received: 17 May 2023
Revised: 2 June 2023
Accepted: 5 June 2023
Published: 6 June 2023

1. Introduction

Short cutting is one of the most commonly used methods of tea reproduction, and the good formation of the adventitious root is a very important matter that involves the survival and cutting seedling formation rate and relates to the success of tea reproduction [1,2]. Adventitious root formation and development of tea cuttings are not only affected by the cuttings themselves (tea varieties, tenderness, etc.) but are also affected by many environmental factors such as light, temperature, humidity, and other external environmental conditions; light (type and duration) is especially important [3]. A previous study found that blue light (430 nm) could rapidly induce adventitious root formation from tea cuttings [4]. In order to further investigate the molecular mechanism of adventitious

root formation and development induced by blue light, time-course sampling of cuttings treated with blue light (450 nm) was performed.

At present, blue light (400–480 nm) has been widely studied on tea plants. For example, under the treatment of blue shading nets, the synthesis of flavonoids and plant hormone signal transduction were regulated [5]. Different intensities of blue light could regulate lipid and flavonoid metabolism, and *CsMYB* might be a hub gene for blue light regulation of lipid and flavonoid metabolism [6]. Zheng et al. (2019) showed that blue light could promote the accumulation of catechins and anthocyanins in tea plants [7]. However, these studies are all about the quality of tea, and there is no report on the study of blue-light-induced adventitious root formation of tea cuttings.

Blue-light-induced root formation has been widely studied in other plants. In the study of *Arabidopsis thaliana*, blue light (470 nm) was able to induce adventitious root formation via the light signal sensor NPH3, and NPH3 regulates adventitious root formation by affecting PIN3-mediated auxin transport [8]. In the study of *Rosmarinus officinalis*, blue light (460 nm) not only significantly induced root formation at the base of cuttings but also induced root formation at the top and middle of cuttings [9]. Blue light also promoted the expression of genes related to IAA biosynthesis. In addition, in the study of *Ocimum basilicum*, blue light (460 nm) was able to rapidly induce root formation in cuttings [10]. These indicated that blue light could positively induce root formation and development, but no relevant time-course analysis has been performed yet.

Phytohormones play an important role in adventitious root formation and the growth of plant cuttings. Previous studies have shown that auxin could greatly promote the rooting efficiency of tea cuttings [1]. Fan et al. (2021) found that the content of indole-3-acetic acid (IAA), salicylic acid (SA), abscisic acid (ABA), and jasmonic acid (JA) in the rootable *C. sinensis* 'Baihaozao' shoots was significantly higher than that in the other two varieties [11]. In addition, light quality can affect phytohormone content. For example, blue light could promote the IAA content of *Picea abies* [12] as well as the ICA, ABA, and JA content of *C. sinensis* [4].

Plant hormone signal transduction plays an essential role in regulating the adventitious root formation and growth of plant cuttings. Wang et al. (2022) showed that *SAUR*, as a hub gene, might play an important role in the adventitious root formation of tea cuttings [2]. Meanwhile, blue light induced root formation of *Ocimum basilicum* cuttings by upregulating the auxin signal [10].

The purpose of this study is to further explore the molecular mechanism of blue-light-induced adventitious root formation and growth of tea cuttings and to look at the potential of optimizing the production of plant material of tea cuttings under blue light. In order to achieve this goal, three objectives were identified: (1) short-term response of tea cuttings to blue light, selecting appropriate lighting time; (2) assessing the dynamic changes in phytohormones in tea cuttings with blue light irradiation time (long-term); (3) identifying the dynamic changes in hormone-related gene expression with blue light irradiation time (long-term). This study revealed the regulatory mechanism of blue light in promoting adventitious root formation and growth of tea cuttings, and it provides new insights for tea breeding.

2. Materials and Methods

2.1. Plant Materials and Light Treatment

The branches of *C. sinensis* 'Jiukengzao' were obtained from the Rizhao Tea Science Research Institute, and they were then cut into cuttings (3–4 cm with a plump axillary bud). The cuttings were inserted into 32-hole plates and were exposed to blue light (450 nm, BL) with a light intensity of 100 μmol m^{-2} s^{-1} and an air humidity of 85 ± 5%. The experiment was established in the artificial climate chamber of the Rizhao Tea Science Research Institute.

2.1.1. Short-Term Treatment

The mature leaves of tea cuttings were sampled at 0 h (control), 8 h, and 16 h (temperature: 25 °C) and were stored in an ultra-low temperature refrigerator at −80 °C for full-length transcriptome sequencing. Each treatment had three replicates.

2.1.2. Long-Term Treatment

The tea short cuttings of *C. sinensis* 'Jiukengzao' (the cutting length was 3–4 cm, and it contained a healthy mature leaf and a plump axillary bud) were exposed to blue light (450 nm, BL) with a light intensity of 100 μmol m^{-2} s^{-1}. Based on short-term treatment transcriptome data, we set the photoperiod to 16 h in the day (25 °C) and 8 h in the night (20 °C). The air humidity was 85 ± 5%. Water was sprayed every 3 d, and they were disinfected with potassium permanganate (in a ratio of 1 mL to 1 L of water) every 15 d. The mature leaves of tea cuttings were sampled at 30, 60, and 90 d of treatment, and they were stored in an ultra-low temperature refrigerator at −80 °C for phytohormone determination and full-length transcriptome sequencing. Each treatment had three replicates.

2.2. Phytohormone Determination

We randomly sampled five mature leaves from each sample, immediately placed them in liquid nitrogen, and then stored them at −80 °C in an ultra-low-temperature refrigerator for backup, with three replicates for each treatment. The 50 g of biological sample stored at ultra-low temperature was taken out and grinded into powder. Then, 10 μL of internal standard mixed solution with a concentration of 100 ng/mL was added. Then, the sample was extracted with 1 mL of methanol/water/formic acid (15:4:1, *v*/*v*/*v*). The mixture was vortexed for 10 min and then centrifugation for 5 min (12,000 r/min and 4 °C). The supernatant was then transferred to clean plastic microtubes, and it was then evaporated to dryness and dissolved in 100 μL of 80% methanol (*V*/*V*). It was then filtered through a 0.22 μm membrane filter. Finally, on the QTRAP6500 + LC-MS/MS platform, MetWare (http://www.metware.cn/, accessed on 12 December 2021) was used to measure phytohormone content. All measurements had three biological replicates.

2.3. RNA Extraction, ONT RNA-Seq, Quality Control, and Full-Length Transcript Identification

We randomly sampled five mature leaves from each sample, immediately placed them in liquid nitrogen, and then stored them at −80 °C in an ultra-low-temperature refrigerator for backup. Using the RNAprep Pure Plant Kit (Tianjin, Beijing, China), RNA was isolated from mature tea leaves under short-term and long-term treatment. Each treatment included three biological repeats. Then, 18 cDNA libraries were constructed using the PCR-cDNA Sequencing Kit (SQK-PCS109) and sequenced on the Nanopore PromethION platform. Full-length transcriptome analysis was conducted by Biomarker Technologies Co., Ltd. (Beijing, China). We filtered ONT RNA-seq raw reads (minimum average read quality score = 6, minimum read length = 350 bp) to remove low-quality reads. Results were mapped to the reference genome *C. sinensis* 'cv.Shuchazao' (CSS_ChrLev, http://tpia.teaplant.org/download.htm, accessed on 12 December 2021). After that, an FLNC transcript cluster was obtained and passed through the Pinfish package within each cluster (https://github.com/nanoporetech/pinfish, accessed on 12 December 2021). After removal, a consistent isomer was obtained. Finally, high-quality isomers were mapped to the reference genome of the tea plant. The cDNA_ Cupcake package was used to further collapse the map reading, with a minimum coverage rate of 85% and a minimum recognition rate of 90%. The 5′ difference was not considered when collapsing redundant transcripts. This produced a full non-redundant transcript.

2.4. Identification and Functional Annotation of Differentially Expressed Genes (DEGs)

Differentially expressed genes (DEGs) were identified from readings from 18 cDNA libraries successfully aligned with the reference genome. Readings with a matching quality higher than 5 were further used for quantification. Gene expression levels were estimated

by counting per million. Using the DESeq R software package (1.18.0), differential expression analysis was performed on leaves under different light qualities. DESeq provides statistical routines for determining differential expression in digital gene expression data using a model based on a negative binomial distribution. The method of Benjamini and Hochberg [13] was used to adjust the generated *p*-value to control the error detection rate. Genes with a *p*-value < 0.05 and foldchange $\geq$ 2 were designated as differentially expressed genes.

Gene functional annotation was based on the following databases: NCBI Non-Redundant Protein Sequences (NR), Protein Families (Pfam), Homologous Clusters of Proteins (KOG/COG/eggNOG), Artificially Annotated and Reviewed Protein Sequence Database (Swiss Prot), Kyoto Encyclopedia of Genes and Genes (KEGG), and Gene Ontology (GO).

2.5. Quantitative Real-Time PCR Analysis

In order to verify the accuracy of transcriptome data, six different genes were randomly selected for expression level verification. Primer Premier 5.0 was used to design primers, and primer sequences are shown in Table S1. Quantitative real-time PCR (qRT-PCR) was performed using 2 × SYBR® Green premixed solution (DF, Beijing, China) on analytikjena-qTOWER2.2 fluorescence quantitative PCR instrument (Jena, Germany). Three biological replicates were analyzed. Glyceraldehyde 3-phosphate dehydrogenase (*CsGAPDH*) was used as a reference gene, and the relative expression was measured by $2^{-\Delta\Delta Ct}$.

2.6. Data Analysis

Statistical analysis was conducted using SPSS 20.0 software (SPSS Inc., Chicago, IL, USA). Single-factor analysis of variance (ANOVA) and Duncan multiple intervals were used to analyze the significant differences between physiological and hormone index data under different light quality treatments. When the *p*-value < 0.05, the differences were considered statistically significant. Graphs were created with Adobe Photoshop CC 2019 and GraphPad Prism.

3. Results

3.1. Selection of Light Time

In order to further determine the light time of long-term treatment, full-length transcriptome sequencing was conducted on mature leaves of cuttings treated with short-term treatment, including 0 h (control), 8 h, and 16 h. See the Appendix A for specific sequencing results.

Previous research showed that auxin transporter protein 1 *AUX1*, auxin early responsive protein *AUX/IAA*, auxin response factor *ARF*, *DELLA*, and protein phosphatase 2C *PP2C* are hub genes that play an important role in promoting adventitious root formation of tea cuttings under blue light. In addition, *PIN1*, *3*, and *4* as well as *PILS6* and *7* also had the highest expression levels under blue light, which might induce the expression of these genes and promote the transportation of ICA from mature leaves to the cutting base, thus promoting adventitious root formation [4]. Therefore, plant hormone signal-transduction-related genes were selected, including four *AUX1s*, four *AUX/IAAs*, five *ARFs*, six *DELLAs*, and two *PP2Cs*. Auxin-transport-related genes were also selected, including *PIN* and *PIN-LIKES* (*PILS*); *PIN* included *PIN1*, *PIN3*, and *PIN4*, and *PILS* included *PILS2*, *PILS6*, and *PILS7*. The expression analysis of these genes showed that except for one *PIN1* and one *PILS7*, the other genes had the highest expression level at 16 h (Figure A2, Table S2). Based on the expression of these genes in this study and our previous research [4], 16 h of light was considered to be more suitable for cutting seedling growth and development, so 16 h of light was used for long-term treatment.

3.2. Phenotypic and Physiological Time-Course Analysis of Tea Cuttings under 16 h of Blue Light Treatment

The tea cutting seedlings were observed after treatment for 30, 60, and 90 d. The results showed that at 30 d, only callus was formed from the cutting seedlings; at 60 d, the cutting seedlings produced a few adventitious roots; and at 90 d, the adventitious roots of cutting seedlings were increased (Figure 1).

Figure 1. Phenotypes of tea cutting seedlings: 30 d, 60 d, and 90 d.

3.3. Phytohormone Time-Course Analysis of Tea Cuttings under 16 h of Blue Light

In order to reveal the internal mechanism of blue-light-induced rooting of tea cutting seedlings, phytohormone determination was conducted on mature leaves of cutting seedlings treated for 30, 60, and 90 d. The results showed that there were significant differences among multiple phytohormones. The descending order of the phytohormones concentrations due to time course were found in abscisic acid (ABA): 60 d > 30 d > 90 d; indole-3-carboxylic acid (ICA): 60 d > 90 d > 30 d; trans-Zeatin (tZ): 90 d > 60 d > 30 d; gibberellin A9 (GA9), and jasmonic acid (JA): 90 d > 30 d > 60 d. In addition, the trend of ICA/tZ and ICA/GA9: 60 d > 90 d > 30 d (Figure 2). These phytohormones played different roles in the process of adventitious root formation induced by blue light in tea cutting seedlings.

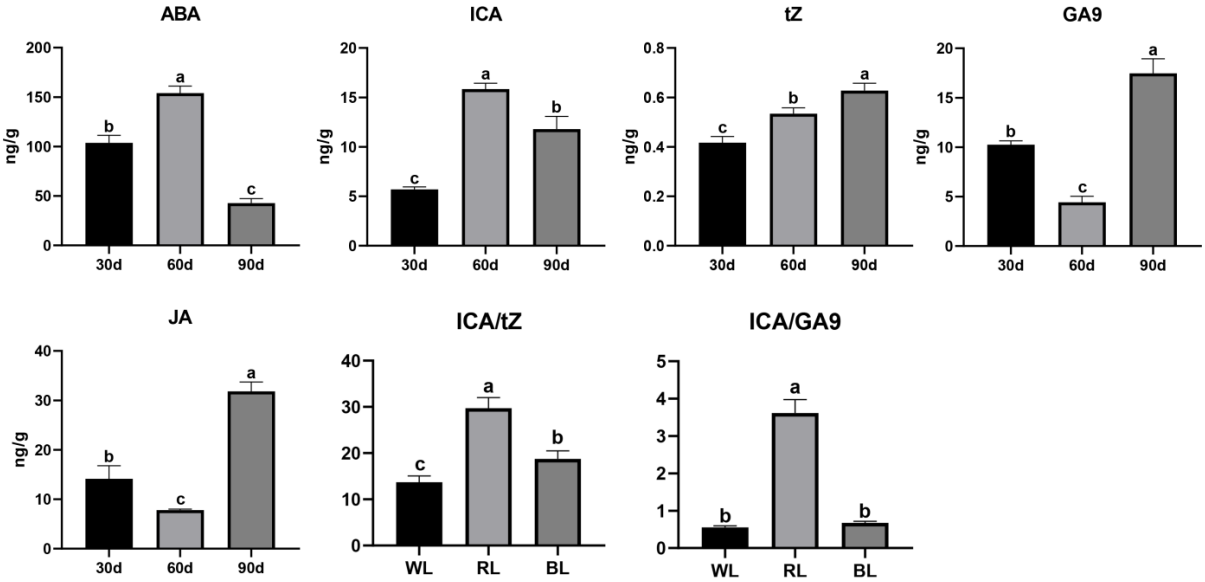

Figure 2. Time-course changes in phytohormone content in mature leaves of tea cutting seedlings: 30 d, 60 d, and 90 d. The *Y*-axis represents the phytohormone content (unit: ng/g). A total of 50 mg of fresh tea leaves per sample were measured. The significance level was ($n = 3$, $p < 0.05$) based on a Duncan multiple intervals significant difference test. Lowercase letters represent significant differences.

3.4. Time-Course Transcriptome of Tea Cuttings under 16 h of Blue Light

In order to study the effect of blue light treatment on gene expression of tea cuttings, nine RNA-seq libraries of *C. sinensis* 'Jiukengzao' were constructed at three light time points: 30 d, 60 d, and 90 d. An average of 5.42 million clean reads were generated per library, and an average of 4.84 million were mapped to the reference genome (Table A2).

Subsequently, using the filter criteria of p-value < 0.05 and foldchange ≥ 2, DEGs were identified by comparing 60 d to 30 d (30 d vs. 60 d) and 90 d to 30 d (30 d vs. 90 d). A total of 1236 DEGs were identified between 30 d and 60 d, of which 557 were significantly upregulated and 679 were significantly downregulated; a total of 2345 DEGs were identified at 30 d vs. 90 d, of which 1555 were significantly upregulated and 790 were significantly downregulated (Figure 3A).

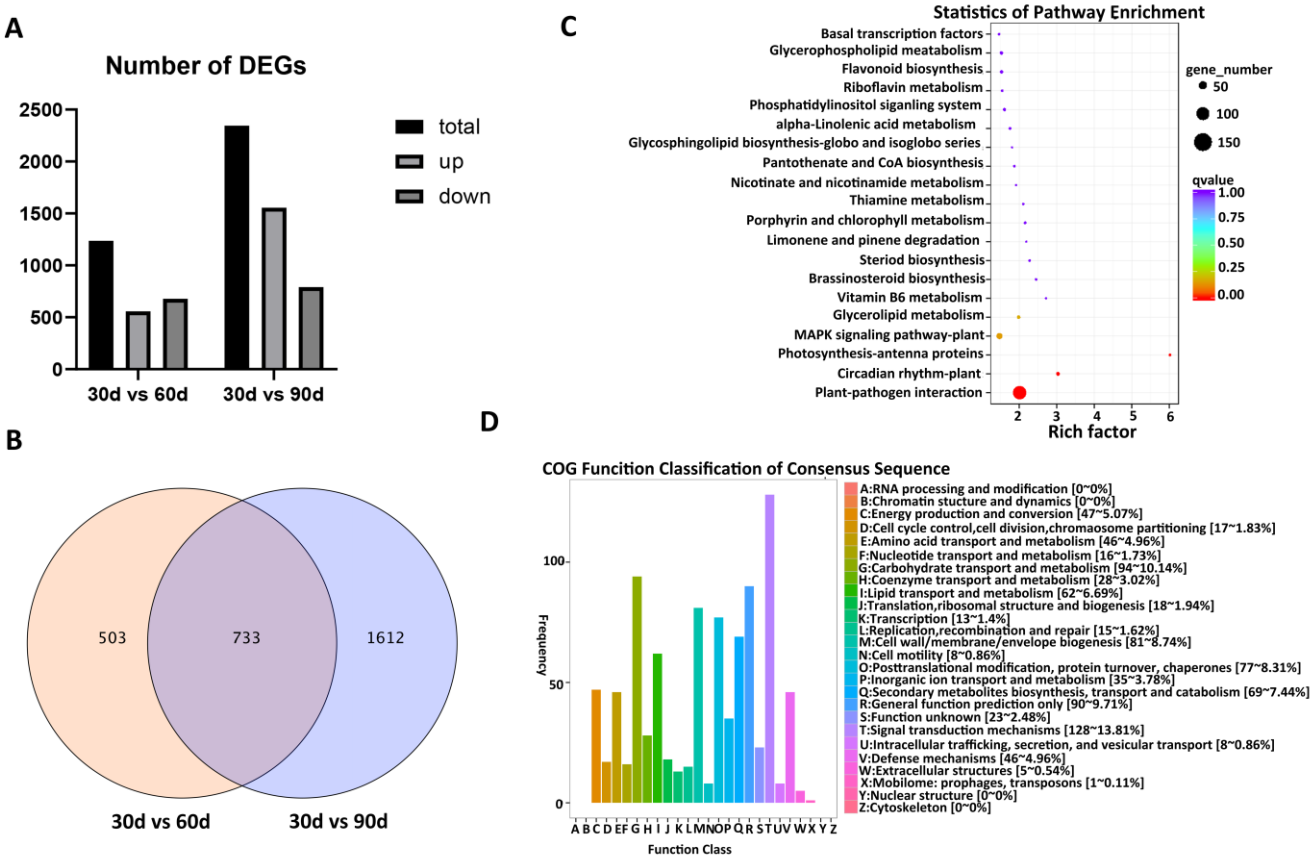

Figure 3. (**A**) Comparison of the number of different genes in mature leaves of tea cutting seedlings under different treatments. The *Y*-axis represents the number of DEGs. (**B**) Venn diagram shows the number of DEGs per comparison between different processes; (**C**) KEGG enrichment map of different genes between different treatments (top 20 statistics of KEGG pathway); (**D**) COG enrichment map of different genes between different treatments.

A total of 2848 DEGs were identified using the two methods, of which 733 genes were common (Figure 3B). Analysis of KEGG pathway enrichment showed that these DEGs are mainly involved in "plant–pathogen interaction (ko04626)", "circadian rhythm-plant (ko04712)", and "photosynthesis-antenna protein (ko00196)" pathways (Figure 3C). COG analysis showed that these DEGs are mainly involved in "signal transduction mechanism" (Figure 3D).

3.5. K-Means Clustering Analysis

The K-means clustering algorithm was used to divide all identified DEGs into 11 clusters. The results showed that the expression trend of genes in K1, K4, and K11

clusters was consistent and gradually decreased, which was contrary to the growth trend of adventitious root of tea cuttings. The expression trend of genes in K2, K5, K6, K7, and K8 clusters was consistent and gradually increased, which was consistent with the growth trend of adventitious root of tea cuttings. The expression trend of genes in K3 and K9 clusters was consistent, increasing first and then decreasing. The expression trend of genes in K10 clustering was decreasing first and then increasing (Figure 4).

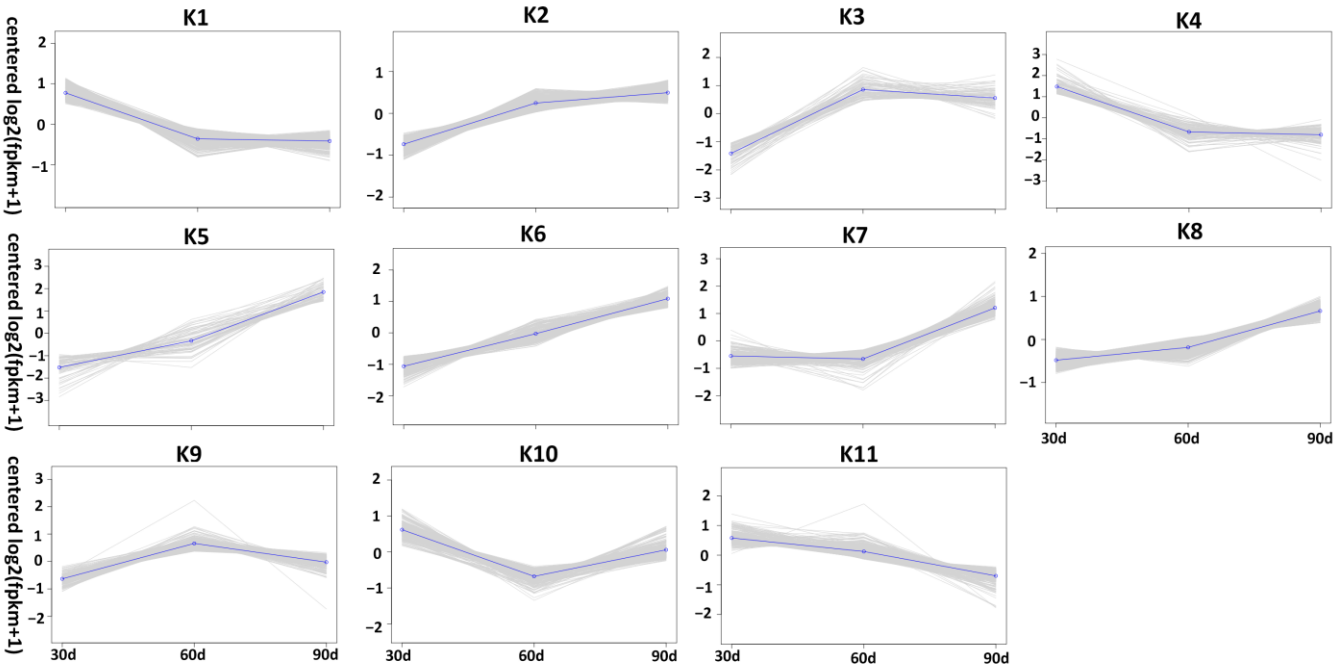

Figure 4. 11 K-means clustering were determined according to the DEG expression level from 30 d to 90 d. Color lines represent the expression trend of genes.

We analyzed the genes in these clusters using KEGG classification. The results indicated that many genes in K1, K4, and K11 clusters were involved in "plant hormone signal transduction (ko04075)", "plant–pathogen interaction (ko04626)", and "circadian rhythm-plant (ko04712)" pathways (Figure S1). Many genes in K2, K5, K6, K7, and K8 clusters were involved in "plant hormone signal transduction (ko04075)" and "plant–pathogen interaction (ko04626)" pathways (Figure S2). Many genes in K3 and K9 clusters were involved in "plant–pathogen interaction (ko04626)" and "circadian rhythm-plant (ko04712)" pathways (Figure S3). Many genes in K10 clusters were involved in "plant hormone signal transduction (ko04075)" and "plant–pathogen interaction (ko04626)" pathways (Figure S4). These pathways might play an important role in blue-light-induced adventitious root growth and development of tea cuttings.

We analyzed the genes in these clusters using COG. The results indicated that many genes in K1, K4, and K11 clusters were involved in "carbohydrate transport and metabolism", "secondary metabolites biosynthesis, transport and catabolism" and "signal transduction mechanisms" (Figure S5). Many genes in K2, K5, K6, K7, and K8 clusters were involved in "signal transduction mechanisms" (Figure S6). Many genes in K3 and K9 clusters were involved in "carbohydrate transport and metabolism" and "signal transduction mechanisms" (Figure S7). Many genes in K10 clusters were involved in "carbohydrate transport and metabolism", "secondary metabolites biosynthesis, transport and catabolism" and "signal transduction mechanisms" (Figure S8). These results indicated that signal transduction might play an important role in blue-light-induced adventitious root growth and development of tea cuttings.

3.6. Analysis of "Plant Hormone Signal Transduction" Pathway

Based on the previous study, plant hormone signal-transduction-related genes were selected and analyzed. Gene expression in K1, K4, and K11 clusters showed a contrary trend to adventitious root growth, while gene expression in K2, K5, K6, K7, and K8 clusters showed a similar trend to adventitious root growth. Therefore, "plant hormone signal transduction" pathway in K1, K4, and K11 as well as K2, K5, K6, K7, and K8 clusters were analyzed.

A total of 12 genes were selected in K1, K4, and K11 clusters, including one *SAUR*, one *CRE1*, three response regulator *B-ARRs*, one *DELLA*, one ethylene receptor *ETR*, two *BRI1s*, one *MYC2*, and one transcription factor *TGA* (Figure 5 and Table S3). The expression of the above genes decreased with the extension of treatment time, which was contrary to the growth trend of the root system.

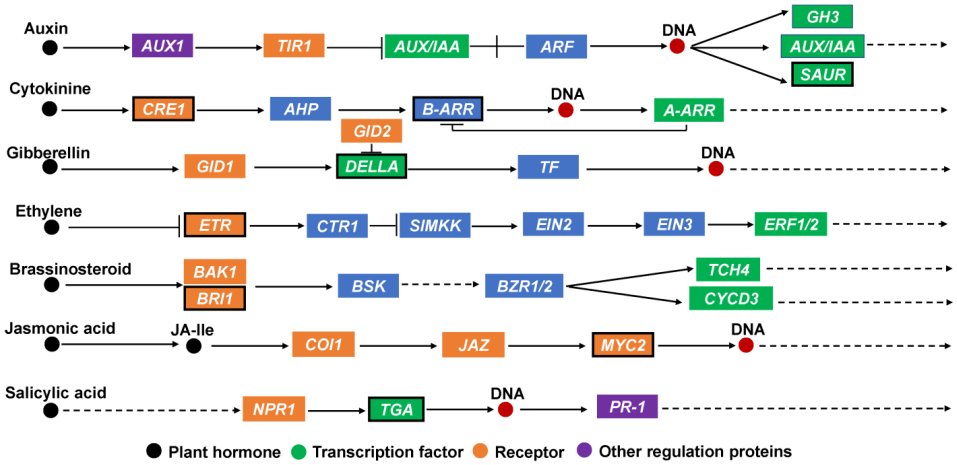

Figure 5. Plant hormone signaling pathways. The genes marked in the black box in the figure were selected from K1, K4, and K11 clusters.

A total of 49 genes were selected in K2, K5, K6, K7, and K8, including one *AUX/IAA*, one *ARF*, four *SAURs*, one gibberellin receptor *GID1*, five *DELLAs*, one abscisic acid receptor *PYR/PYL*, one serine/threonine protein kinase CTR1, two mitogen-activated protein kinase kinase *SIMKKs*, sixteen brassinosteroid-insensitive 1-associated receptor kinase 1 *BAK1s*, ten protein brassinosteroid-insensitive 1 *BRI1s*, four jasmonate ZIM domain-containing protein *JAZs*, two transcription factor *MYC2s*, and one regulatory protein *NPR1* (Figure 6, Table S3). The expression of the above genes increased with the extension of treatment time, which was consistent with the growth trend of the root system.

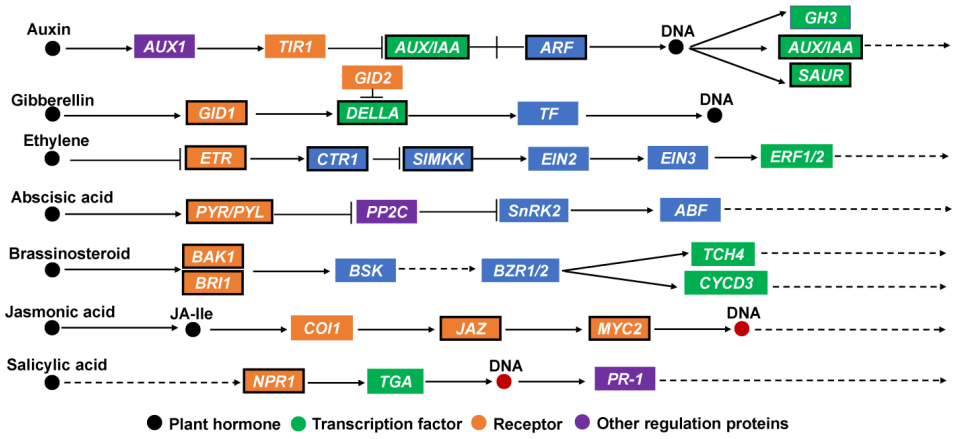

Figure 6. Plant hormone signaling pathways. The genes marked in the black box in the figure were selected from K2, K5, K6, K7 and K8 clusters.

3.7. Identification of Auxin Synthesis and Transportation-Related Genes

According to the results of the identification of auxin synthesis and transportation-related genes, two major categories of auxin-transport-related genes were identified, including *PIN* and *PIN-LIKES (PILS)*. The *PIN* includes one *PIN1*, one *PIN3*, and one *PIN4*, and the *PILS* includes one *PILS2*, one *PILS6*, and two *PILS7s*. The expression analysis of these genes showed that the expression trend of most genes (except for one *PILS2* and one *PILS6*) was: 60 d > 90 d > 30 d (Figure 7A, Table S4).

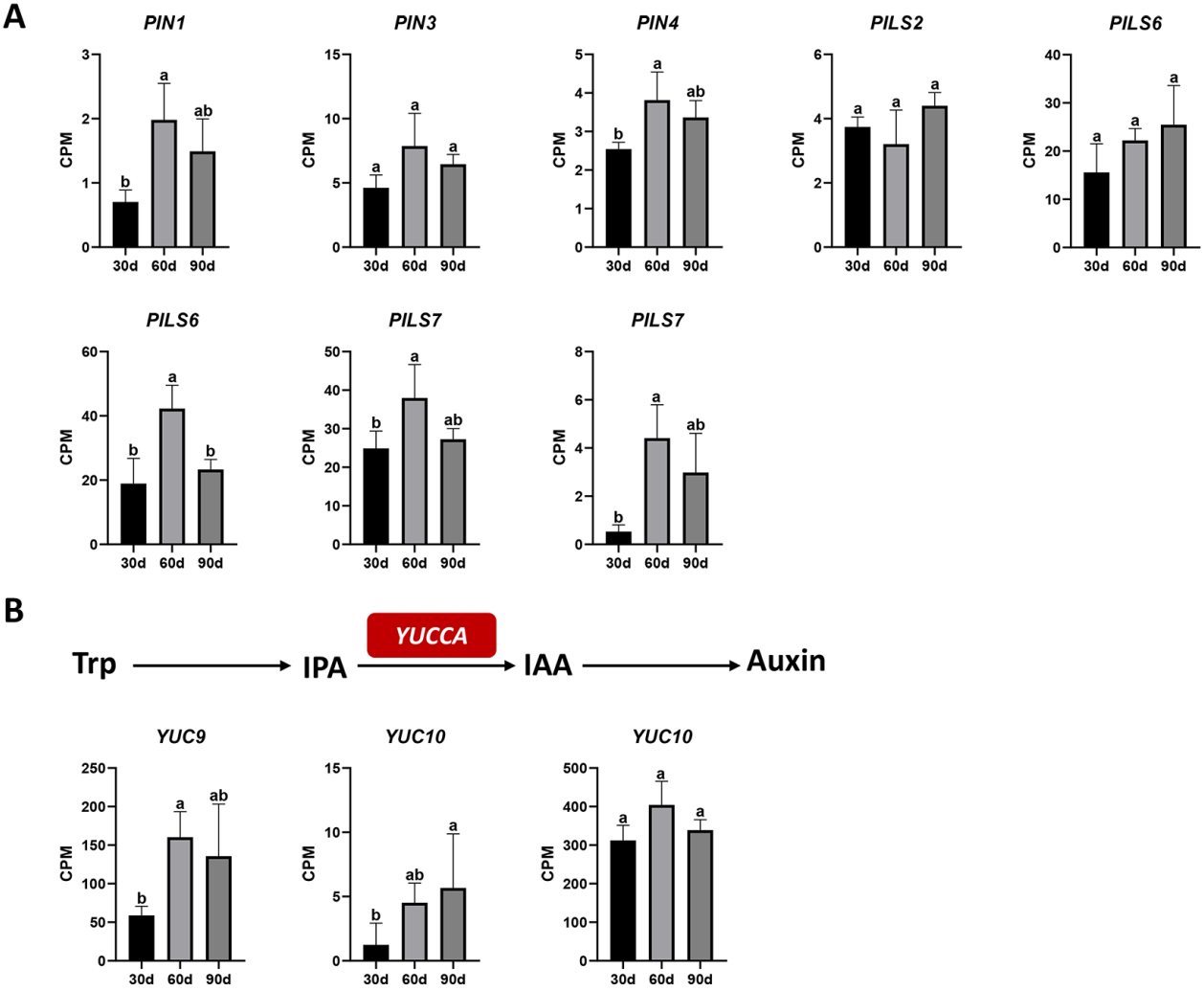

Figure 7. (**A**) G Expression level of genes related to auxin transport. (**B**) Expression level of genes related to auxin synthesis. The *Y*-axis represents the expression level of genes represented by counts per million (CPM). The significance level was (n = 3, $p < 0.05$) based on a Duncan multiple intervals significant difference test. Lowercase letters represent significant differences.

A total of three flavin monooxygenase genes *YUC* were identified, including one *YUC9* and two *YUC10s*. Expression analysis of these genes showed that the expression trend of these three genes was: 60 d > 90 d > 30 d (Figure 7B, Table S5).

3.8. Validation of Genes by qRT-PCR

To verify the reliability of full-length transcriptome data, six genes were randomly selected for qRT-PCR validation. The results showed that the expression trend of most genes was consistent with the relative expression in qRT-PCR (Figure 8), proving that full-length transcriptome data is reliable and can be used for future research.

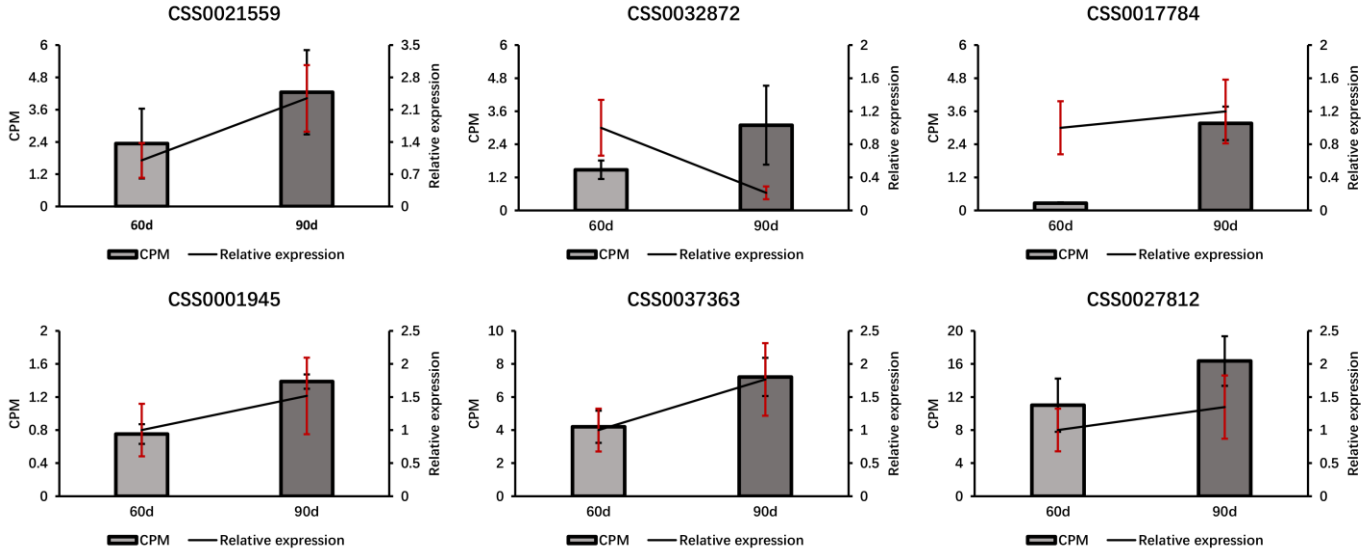

Figure 8. qRT-PCR validation results using *CsGAPDH* as an internal control. The left *Y*-axis represents counts per million (CPM) values for Oxford Nanopore Technologies (ONT) RNA-Seq, and the right *Y*-axis represents relative qRT-PCR expression levels (the relative expression was measured by $2^{-\Delta\Delta Ct}$). In the figure, the bars represent ONT RNA-Seq, and the lines represent qRT-PCR.

4. Discussion

4.1. Blue Light Induced Adventitious Root Development by Affecting Phytohormone Content

A lot of evidence shows that endogenous phytohormones play an important role in adventitious root formation and development [14–16]. ICA belongs to auxin. In this study, the content of ICA increased first and then decreased with time (Figure 2). This indicated that 30 to 60 d might be a high-incidence period for adventitious root formation. During this time, tea cuttings needed to transport more ICA from mature leaves to the base of cuttings, so the content increased. From 60 to 90 d, adventitious root formed and could produce ICA for their growth and development, the demand for ICA in mature leaves was reduced, so the content was decreased. ABA was considered an inhibitor of the rooting of *Eucalyptus globulus* [17], but in this study, its content also increased first and then decreased, increasing during the rooting period (Figure 2). In addition, in previous studies, ABA had the highest content under blue light, which was most favorable for rooting [4] and was highest in the new shoots of the easily rooted *C. sinensis* 'Baihaozao' [11]. These differences may be related to the different ABA distribution in different tissues, and the ABA metabolism in mature leaves is not the same as the base of cuttings. In addition, McAdam et al. (2016) reported that shoot-derived ABA could promote root growth [18]. In this study, the changing trend of GA9 and JA content was consistent, decreasing first and then increasing (Figure 2). As an inhibitor of adventitious root formation, GA content decreased during adventitious root formation but increased later, and this might be because the adventitious root has formed, and GA9 has no effect on the adventitious root growth. In addition, the ratio of ICA/GA9 showed a trend of first increasing and then decreasing (Figure 2). Fan et al.'s (2021) study showed that the IAA/GA3 ratio in the new shoots of the best rooting *C. sinensis* 'Baihaozao' was significantly higher than other varieties [11], which also explains the reason for the increase in ICA/GA9 ratio in the early stage (Figure 2). JA can rapidly accumulate in the rooting induction stage of *Petunia hybrida* cuttings [19], which indicates that JA can promote adventitious root formation. However, in this study, during adventitious root formation, JA content showed a downward trend and later increased. This might be due to the dominant role of ICA during adventitious root formation. tZ belongs to the cytokinin class, and its content gradually increased in this study. However, the ratio of ICA/tZ showed a trend of first increasing and then decreasing. It has been

proven that the high ratio of auxin to cytokinin in vivo promotes root formation [1], which might be the reason for the increase in ICA/tZ ratio between 30 and 60 d.

4.2. Blue Light Induced Adventitious Root Development in Tea Cuttings by Affecting Auxin Synthesis

Auxin can promote cell division and differentiation, increase the number of cells, and promote adventitious roots formation and development in cuttings. ICA belongs to the auxin category. In this study, the content of ICA was: 60 d > 90 d > 30 d (Figure 2). The synthesis of auxin is achieved through tryptophan (Trp)-dependent and independent methods, with Trp-dependent methods being much better [20]. Among the Trp-dependent pathways, indole pyruvic acid (IPyA) is the most important, including the two-step reaction of converting Trp to IAA, in which *YUC* catalyzes an irreversible reaction: the oxidative decarboxylation of IPyA to form IAA [20–23]. In this study, the expression trend of *YUC* was: 60 d > 90 d > 30 d (Figure 7B). In our previous research, ICA had the highest content under blue light, which promoted the best rooting, and *YUC* was also expressed at the highest level under blue light [4]. The above results indicated that *YUC* might play an important role in blue-light-induced ICA synthesis.

4.3. Blue Light Induced Adventitious Root Development in Tea Cuttings by Affecting Expression of PIN and PILS Genes

At the early stage of cutting, there are no adventitious roots at the base of the cutting, and the auxin required for adventitious root formation is synthesized from mature leaves and transported to the base of the cutting. Currently, the main auxin transport carriers found are AUXIN1/LIKE-AUX1 (AUX/LAX), PIN-FORMED (PIN), and the ATP-binding cassette subfamily B (ABCB) family, in which AUX/LAX is an inner flow carrier and PIN and ABCB are outer flow carriers [24]. PIN-LIKES (PILS) has been identified as a new auxin-transport-promoting factor family. It has been demonstrated through cell sensitivity to auxin that PILS protein is necessary for auxin-dependent regulation of plant growth [25].

Auxin is a positive regulator during root development, and its transport is crucial [26,27]. Previous studies have shown that during the long-distance transportation of auxin from stem tip to root, *PIN7* and *ABCB1* are expressed at the stem tip and are responsible for the loading of auxin, while *PIN1* and *ABCB19* are responsible for maintaining the flow of auxin from stem to root [28–30]. This indicates that *PIN1* can promote the transportation of auxin from the aboveground part to the underground part, thereby promoting the growth and development of the root system. At the same time, auxin efflux vector mutants such as *PIN* exhibit severe root defects [26]. *AtPIN3* participates in the early formation of lateral roots, and *AtPIN4* also plays an important role in root development [31–34]. In addition, studies have reported that the formation of adventitious roots in *Arabidopsis* induced by blue light is regulated by *PIN3*-mediated auxin transport. Blue light improved the content of auxin in adventitious roots, and the *PIN3* protein level of blue light treatment was higher than that of dark conditions [8]. In this study, the expression trend of *PIN1*, *PIN3*, and *PIN4* was 60 d > 90 d > 30 d (Figure 7A), which is consistent with the change trend of ICA content. In our previous study, *PIN1*, *3*, and *4* had the highest expression levels under blue light [4]. This indicated that the expression of *PIN* gene was related to the content of auxin. In the research of tea plants, the *CsPIN3* gene has been proven to be involved in regulating the growth and development of adventitious roots and the accumulation of auxin [35]. In summary, these results indicated that blue light promoted the transport of auxin from mature leaves to the base of cuttings by regulating the expression of *PIN* genes, thereby inducing adventitious root formation.

PILS proteins act as auxin carriers in the endoplasmic reticulum (ER), where they can stimulate intracellular auxin accumulation [25]. It has been proven that *AtPILS1-7* are responsible for auxin polar transport and determine the direction in which auxin flows through the tissue [36]. Research has reported that *PILS6* can control the nuclear abundance of auxin to regulate auxin response and subsequent root growth [37]. In the study of tea plants, *CsPILS* played an important role in the adventitious root formation

process of cutting seedlings [35]. In this study, the expression trend of *PILS6* and *PILS7* was 60 d > 90 d > 30 d (Figure 7A), which is consistent with the change trend of ICA content. In our previous study, *PILS6* and *7* had the highest expression levels under blue light [4]. The above results indicated that blue light promoted the transport of auxin from mature leaves to the base of cuttings by regulating the expression of *PILS* genes, thereby inducing adventitious root formation and development.

4.4. Blue Light Induced Adventitious Root Development in Tea Cuttings by Affecting Expression of Hormone Signal-Transduction-Related Genes

The development of adventitious and lateral roots in plants is regulated by auxin [32]. Plants can quickly respond to changes in auxin levels through auxin-response factors such as *AUX/IAA*, *ARF*, *SAUR*, and *GH3* [38–40]. *IAA17* is involved in some typical phenotypes of auxin signal transduction control, such as adventitious root and root hair formation [41,42]. Study has shown that signal transduction mediated by *AUX/IAA* and *ARF* played an important role in regulating plant root formation [41]. *ZmIAA10* can interact with *ZmARF25* and *34*, thereby affecting the root growth and development of *Zea mays* [43]. In this study, the expression trend of *AUX/IAA* and *ARF* is consistent (Figure 6), indicating that there may be a synergistic effect between *AUX/IAA* and *ARF* in blue-light-induced adventitious root formation. In addition, in the study of *Arachis hypogaea*, the expression level of *AhARF14/26/45* was positively correlated with root length, root surface area, and root tip number [44]. In the study of *Arabidopsis*, overexpression of *SAUR76* promoted taproot elongation [45]. In this study, the expression levels of *AUX/IAA*, *ARF*, and *SAUR* increased with the prolongation of treatment time, which had the same trend as the root formation and growth (Figure 6). In addition, *AUX/IAA*, *ARF*, and *SAUR* act as hub genes, which had the highest expression levels under blue light in our previous study [4]. The above results indicated that *AUX/IAA*, *ARF*, and *SAUR* played important roles in adventitious root formation and development of tea cuttings induced by blue light.

In addition to auxin signal pathway involved in blue-light-induced adventitious roots, other hormone signal pathways were also involved, including gibberellin, abscisic acid, ethylene, brassinolide, jasmonic acid, and salicylic acid signal pathways. Fan et al. (2021) conducted a study on three cutting seedlings with different rooting abilities, indicating that the expression of *DELLA* in the shoots of *C. sinensis* 'Baihaozao' with the best rooting ability was higher than that of the other two varieties [11]. In addition, *DELLA* expression increased during the adventitious root formation of *Populus*, which is similar to the results of the current research [46]. *PYR/PYL* can promote PP2A activity, thus eliminating PINIOD (PID)-mediated phosphorylation of PIN protein, which facilitates auxin efflux transport and maintains normal root development [47]. In this study, the expression of *PYR/PYL* increased with treatment time (Figure 6), indicated that it might play an important role in the process of blue-light-induced adventitious root growth and development. *CRE1*, as a cytokinin receptor, and *B-ARR*, as a positive regulatory factor for cytokinin, gradually decreased in expression (Figure 5). Previous research has shown that *MtCRE1* negatively regulates root growth and development [48]. At the same time, in the study of *Populus*, *PtRR13* (*B-ARR*) was considered a negative regulator of the adventitious root [49]. In summary, blue light might promote adventitious root formation and growth of tea cuttings by regulating the expression of *DELLA*, *PYR/PYL*, *B-ARR*, and *CRE1*.

Brassinolide (BR) signal transduction can influence many plant processes, including nutrition and reproductive growth, root growth, and photomorphogenesis. *BAK1* is the receptor gene of BR, and the up-regulated expression of *BAK1* can promote the root growth of *Brassica napus* [50], which proves that *BAK1* may have a positive response to root growth. At the same time, in the study of *Cucumis sativus*, the upregulated expression of *BAK1* had a positive regulatory effect on the adventitious root [51]. In the study of *Arabidopsis*, the expression of *BRI1* rescued the root growth of the *bri1* mutant [52,53], indicating that *BRI1* was positively regulating root growth. In this study, the expression levels of multiple *BAK1* and *BRI1* increased with adventitious root growth, which indicated that blue light might

promote tea cutting adventitious root growth and development by inducing the expression of *BAK1* and *BRI1*. JA regulates plant growth and development, including root growth, flowering, etc. As the response factors of JA, *JAZ* and *MYC2* expression levels increased and decreased, respectively, with the prolongation of blue light irradiation time. In the study of *Arabidopsis*, *JAZ4* has been shown to promote root elongation [54]. In the study of *Populus*, transgenic methods were used to prove that *PttMYC2* has negative effects on the adventitious root [55], and *AtMYC2* has also been proved to be a negative regulator of adventitious root development in *Arabidopsis* [56,57]. In conclusion, blue light might induce the adventitious root formation and development by regulating the expression of *BAK1*, *BRI1*, *JAZ*, and *MYC2*.

5. Conclusions

This study further explored the molecular mechanism of adventitious root formation and development in tea cuttings induced by blue light through time-course analysis. We draw the following conclusion: (1) based on the full-length transcriptome results (short-term), we further determined that 16 h of light was suitable for adventitious root formation and growth of tea cuttings. (2) Long-term processed phytohormone data indicated that the change in ICA content was: 60 d > 90 d > 30 d. (3) According to our long-term full-length transcriptome analysis, blue light induced adventitious root formation and growth of tea cuttings by promoting the expression of hormone signal transduction, auxin synthesis, and transportation-related genes such as *AUX/IAA*, *ARF*, *SAUR*, *YUC*, *PIN*, and *PILS*. In conclusion, our research laid a foundation for future research on the impact of blue light on tea growth and development, and it also provided a theoretical basis for supplementing blue light to induce adventitious root formation in actual production.

Supplementary Materials: The following supporting information can be downloaded at: https://www.mdpi.com/article/10.3390/agronomy13061561/s1, Table S1: Primers used for real-time PCR analysis; Table S2: Annotation of short-term plant hormone signal-transduction-related genes; Table S3: Annotation of long-term plant hormone signal-transduction-related genes; Table S4: Annotation of auxin-transport-related genes; Table S5: Annotation of auxin-synthesis-related genes. Figure S1: KEGG classification diagram of genes in K1, K4, and K11 clusters; Figure S2: KEGG classification diagram of genes in K2, K6, K7, and K8 clusters; Figure S3: KEGG classification diagram of genes in K3 and K9 clusters; Figure S4: KEGG classification diagram of genes in K10 cluster; Figure S5: COG classification diagram of genes in K1, K4, and K11 clusters; Figure S6: COG classification diagram of genes in K2, K6, K7, and K8 clusters; Figure S7: COG classification diagram of genes in K3 and K9 clusters; Figure S8: COG classification diagram of genes in K10 cluster.

Author Contributions: Y.S. conducted experiments, analyzed the data, and wrote the manuscript. H.W. conducted experiments, collected samples, and statistically analyzed data. X.H. participated in manuscript writing and picture production. Z.D., K.F. and Y.W. participated in the experimental design and revised the manuscript. J.S. revised the manuscript. H.L., S.D. and D.S. collected samples. All authors have read and agreed to the published version of the manuscript.

Funding: This research was funded by the Technology System of Modern Agricultural Industry in Shandong Province (SDAIT19-01) and the Special Foundation for Distinguished Taishan Scholar of Shandong Province (ts201712057), the Project of Agricultural Science and Technology Fund in Shandong Province (2019LY002, 2019YQ010, and 2019TSLH0802), Shandong Agricultural Seed Improvement Project (2020LZGC010), the Project of Rizhao Natural Science Foundation Youth Fund (RZ2021ZR48), the Livelihood Project of Qingdao City (22-3-7-xdny-5-nsh), and the Agricultural Science and Technology Innovation Project of Shandong Academy of Agricultural Sciences (CXGC2023F18, CXGC2023A11).

Data Availability Statement: The raw data for RNA-seq have been uploaded to the NCBI SRA with accession number PRJNA948654.

Acknowledgments: We thank the whole research group for their active role in the experimental process, data analysis, and manuscript revision.

Conflicts of Interest: The authors declare no conflict of interest.

Appendix A

A total of 9 ONT RNA-seq libraries of C.Jiukengzhao were constructed, each library generating an average of 6.34 million clean reads, with more than 90% being mapped to the reference genome (Table A1).

DEGs were identified using the methods of 8 h vs. 0 h (0 h vs. 8 h) and 16 h vs. 0 h (0 h vs. 16 h). A total of 1448 DEGs were identified during 0 h vs. 8 h, of which 817 were significantly up-regulated and 631 were significantly down-regulated (Figure A1A). KEGG enrichment analysis showed that many DEGs were significantly enriched in "photosynthesis-antenna proteins (ko00196)", "circadian rhythm-plant (ko04712)", and "glutathione metabolism (ko00480)" (Figure A1B). A total of 4299 DEGs were identified between 0 h and 16 h, of which 2195 were significantly up-regulated and 2104 were significantly down-regulated (Figure A1C). KEGG enrichment analysis showed that many DEGs were significantly enriched in "ribosome (ko03010)", "circadian rhythm-plant (ko04712)", and "glutathione metabolism (ko00480)" (Figure A1D).

890 DEGs identified in 0 h vs. 8 h and 0 h vs 16 h were common (Figure A1E). KEGG enrichment analysis was performed on these genes. The results showed that many DEGs were significantly enriched in "ribosome (ko03010)", "circadian rhythms-plant (ko04712)", "photosynthesis-antenna proteins (ko00196)", and "glutathione metabolism (ko00480)" (Figure A1F).

Table A1. Overview of transcriptome data.

Sample ID	Number of Clean Reads (Except rRNA)	Number of Full-Length Reads	Full-Length Percentage (FL%)
0h_1	6,383,327	5,832,344	91.37%
0h_2	6,281,373	5,665,386	90.19%
0h_3	6,501,101	5,891,757	90.63%
8h_1	5,960,317	5,405,466	90.69%
8h_2	6,158,486	5,553,751	90.18%
8h_3	6,799,050	6,224,172	91.54%
16h_1	6,847,326	6,213,137	90.74%
16h_2	5,748,251	5,174,767	90.02%
16h_3	6,400,329	5,788,703	90.44%
total	57,079,560		
average	6,342,173		

Table A2. Overview of transcriptome sequencing.

Sample ID	Number of Clean Reads (Except rRNA)	Number of Full-Length Reads	Full-Length Percentage (FL%)
30d_1	5,025,914	4,509,142	89.72%
30d_2	5,299,175	4,748,264	89.60%
30d_3	5,411,112	4,857,789	89.77%
60d_1	6,560,599	5,877,347	89.59%
60d_2	5,677,068	5,132,504	90.41%
60d_3	4,438,631	3,999,763	90.11%
90d_1	5,334,681	4,340,179	81.36%
90d_2	5,052,951	4,595,471	90.95%
90d_3	6,035,357	5,527,896	91.59%
total	48,835,488		
average	5,426,165		

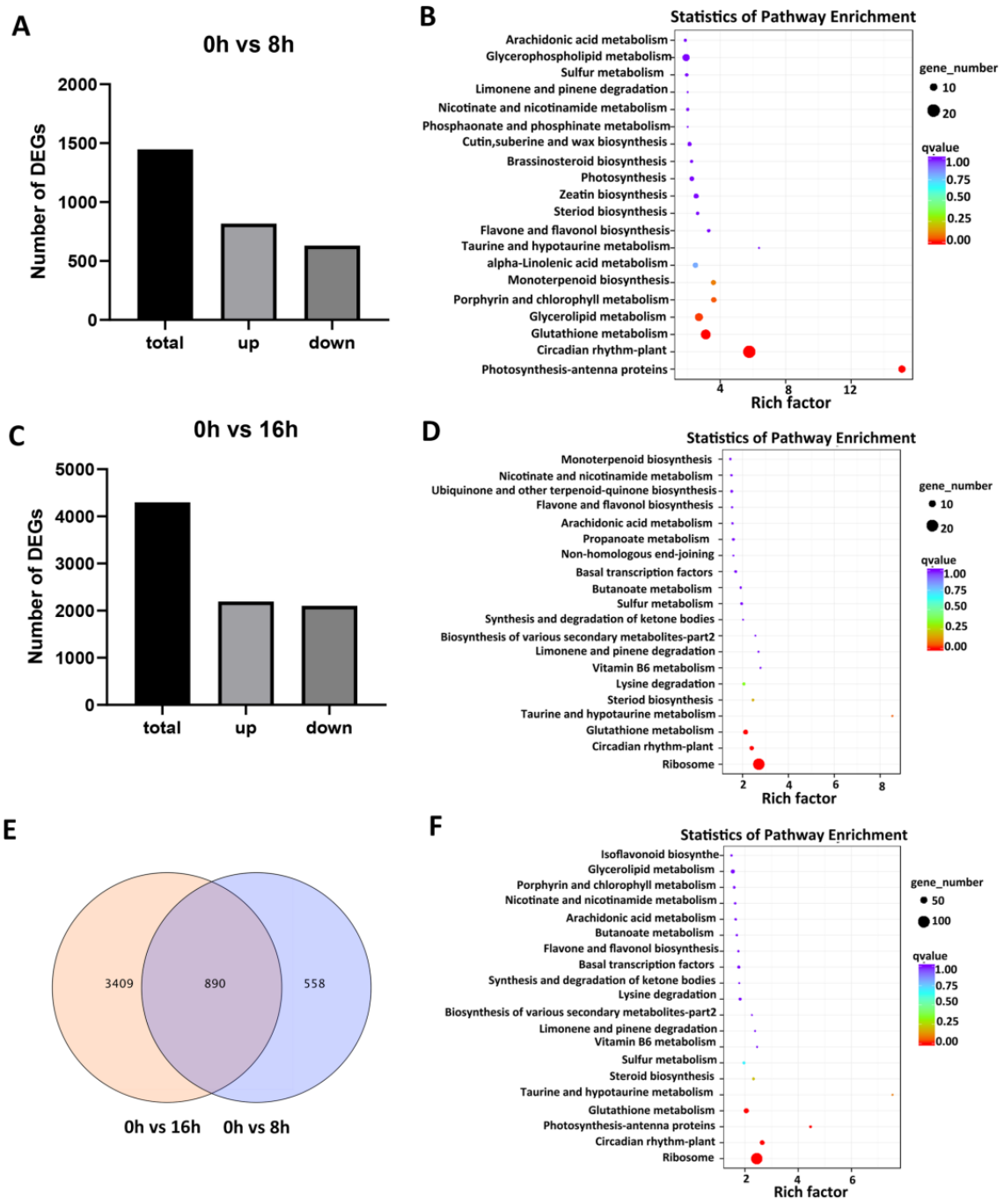

Figure A1. (**A**) Number of DEGs identified in 0 h vs. 8 h, The Y-axis represents the number of DEGs; (**B**) KEGG enrichment map of DEGs in 0 h vs. 8 h (Top 20 statistics of KEGG pathway); (**C**) number of DEGs identified at 0 h vs. 16 h, The Y-axis represents the number of DEGs; (**D**) KEGG enrichment map of DEGs in 0 h vs. 16 h (Top 20 statistics of KEGG pathway); (**E**) The VENN diagram of pairwise comparison; (**F**) KEGG enrichment map of all DEGs (Top 20 statistics of KEGG pathway).

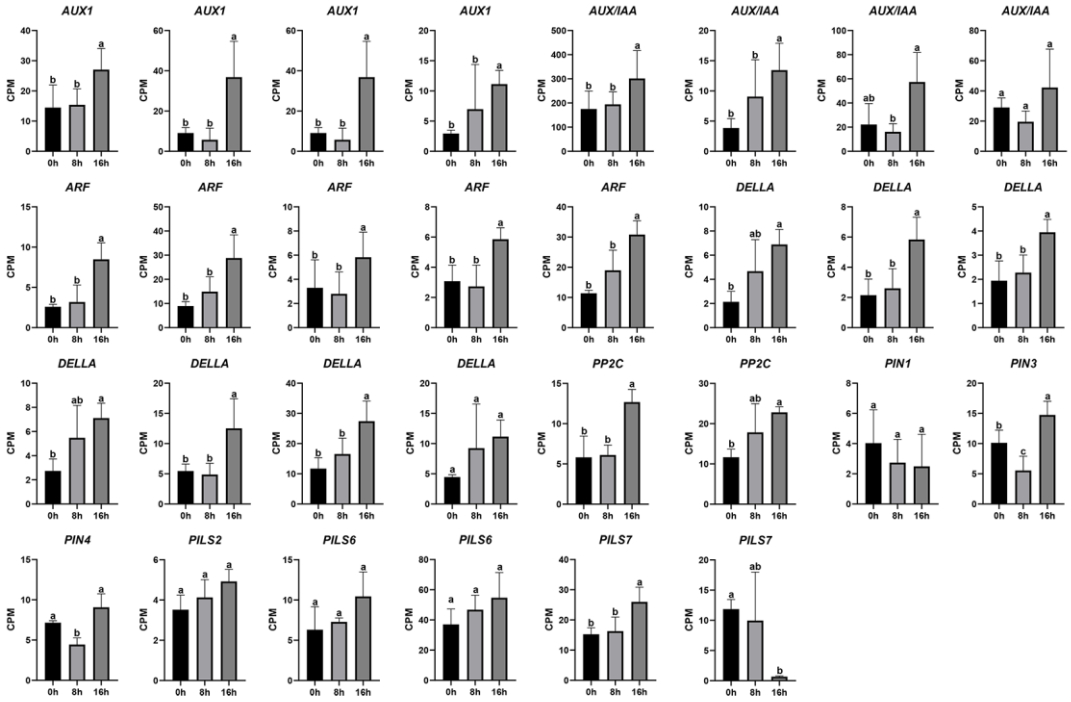

Figure A2. Expression map of genes associated with plant hormone signal transduction and auxin transport (CPM). The *Y*-axis represents the expression level of genes (CPM). Lowercase letters represent significant differences.

References

1. Wei, K.; Ruan, L.; Wang, L.; Cheng, H. Auxin-Induced Adventitious Root Formation in Nodal Cuttings of *Camellia sinensis*. *Int. J. Mol. Sci.* **2019**, *20*, 4817. [CrossRef] [PubMed]
2. Wang, Y.; Pang, D.; Ruan, L.; Liang, J.; Zhang, Q.; Qian, Y.; Zhang, Y.; Bai, P.; Wu, L.; Cheng, H.; et al. Integrated transcriptome and hormonal analysis of naphthalene acetic acid-induced adventitious root formation of tea cuttings (*Camellia sinensis*). *BMC Plant Biol.* **2022**, *22*, 319. [CrossRef] [PubMed]
3. Proebsting, W.M. Plant Propagation: Principles and Practices. *For. Sci.* **1984**, *30*, 156.
4. Shen, Y.; Fan, K.; Wang, Y.; Wang, H.; Ding, S.; Song, D.; Shen, J.; Li, H.; Song, Y.; Han, X.; et al. Red and Blue Light Affect the Formation of Adventitious Roots of Tea Cuttings (*Camellia sinensis*) by Regulating Hormone Synthesis and Signal Transduction Pathways of Mature Leaves. *Front. Plant Sci.* **2022**, *13*, 2398. [CrossRef] [PubMed]
5. Ye, J.H.; Lv, Y.Q.; Liu, S.R.; Jin, J.; Wang, Y.F.; Wei, C.L.; Zhao, S.Q. Effects of Light Intensity and Spectral Composition on the Transcriptome Profiles of Leaves in Shade Grown Tea Plants (*Camellia sinensis* L.) and Regulatory Network of Flavonoid Biosynthesis. *Molecules* **2021**, *26*, 5836. [CrossRef]
6. Wang, P.; Chen, S.; Gu, M.; Chen, X.; Chen, X.; Yang, J.; Zhao, F.; Ye, N. Exploration of the Effects of Different Blue LED Light Intensities on Flavonoid and Lipid Metabolism in Tea Plants via Transcriptomics and Metabolomics. *Int. J. Mol. Sci.* **2020**, *21*, 4606. [CrossRef]
7. Zheng, C.; Ma, J.-Q.; Ma, C.-L.; Shen, S.-Y.; Liu, Y.-F.; Chen, L. Regulation of Growth and Flavonoid Formation of Tea Plants (*Camellia sinensis*) by Blue and Green Light. *J. Agric. Food Chem.* **2019**, *67*, 2408–2419. [CrossRef]
8. Zhai, S.; Cai, W.; Xiang, Z.-X.; Chen, C.-Y.; Lu, Y.-T.; Yuan, T.-T. PIN3-mediated auxin transport contributes to blue light-induced adventitious root formation in Arabidopsis. *Plant Sci.* **2021**, *312*, 111044. [CrossRef]
9. Gil, C.-S.; Kwon, S.-J.; Jeong, H.-Y.; Lee, C.; Lee, O.-J.; Eom, S.-H. Blue Light Upregulates Auxin Signaling and Stimulates Root Formation in Irregular Rooting of Rosemary Cuttings. *Agronomy* **2021**, *11*, 1725. [CrossRef]
10. Lim, Y.J.; Eom, S.H. Effects of different light types on root formation of *Ocimum basilicum* L. cuttings. *Sci. Hortic.* **2013**, *164*, 552–555. [CrossRef]
11. Fan, K.; Shi, Y.; Luo, D.; Qian, W.; Shen, J.; Ding, S.; Ding, Z.; Wang, Y. Comparative Transcriptome and Hormone Analysis of Mature Leaves and New Shoots in Tea Cuttings (*Camellia sinensis*) among Three Cultivars with Different Rooting Abilities. *J. Plant Growth Regul.* **2021**, *41*, 2833–2845. [CrossRef]
12. Ouyang, F.; Mao, J.-F.; Wang, J.; Zhang, S.; Li, Y. Transcriptome Analysis Reveals that Red and Blue Light Regulate Growth and Phytohormone Metabolism in Norway Spruce [*Picea abies* (L.) Karst.]. *PLoS ONE* **2015**, *10*, e0127896. [CrossRef]
13. Westfall, P.H. The Benjamini-Hochberg method with infinitely many contrasts in linear models. *Biometrika* **2008**, *95*, 709–719. [CrossRef]

14. da Costa, C.T.; de Almeida, M.R.; Ruedell, C.M.; Schwambach, J.; Maraschin, F.D.S.; Fett-Neto, A.G. When stress and development go hand in hand: Main hormonal controls of adventitious rooting in cuttings. *Front. Plant Sci.* **2013**, *4*, 133. [CrossRef]
15. Druege, U.; Hilo, A.; Pérez-Pérez, J.M.; Klopotek, Y.; Acosta, M.; Shahinnia, F.; Zerche, S.B.; Franken, P.; Hajirezaei, M.R. Molecular and physiological control of adventitious rooting in cuttings: Phytohormone action meets resource allocation. *Ann. Bot.* **2019**, *123*, 929–949. [CrossRef]
16. Gonin, M.; Bergougnoux, V.; Nguyen, T.D.; Gantet, P.; Champion, A. What Makes Adventitious Roots? *Plants* **2019**, *8*, 240. [CrossRef]
17. Negishi, N.; Nakahama, K.; Urata, N.; Kojima, M.; Sakakibara, H.; Kawaoka, A. Hormone level analysis on adventitious root formation in *Eucalyptus globulus*. *New For.* **2014**, *45*, 577–587. [CrossRef]
18. McAdam, S.A.M.; Brodribb, T.J.; Ross, J.J. Shoot-derived abscisic acid promotes root growth. *Plant Cell Environ.* **2016**, *39*, 652–659. [CrossRef]
19. Lischweski, S.; Muchow, A.; Guthörl, D.; Hause, B. Jasmonates act positively in adventitious root formation in petunia cuttings. *BMC Plant Biol.* **2015**, *15*, 229. [CrossRef]
20. Zhao, Y. Essential Roles of Local Auxin Biosynthesis in Plant Development and in Adaptation to Environmental Changes. *Annu. Rev. Plant Biol.* **2018**, *69*, 417–435. [CrossRef]
21. Casanova-Sáez, R.; Voß, U. Auxin Metabolism Controls Developmental Decisions in Land Plants. *Trends Plant Sci.* **2019**, *24*, 741–754. [CrossRef] [PubMed]
22. Zheng, Z.; Guo, Y.; Novák, O.; Dai, X.; Zhao, Y.; Ljung, K.; Noel, J.P.; Chory, J. Coordination of auxin and ethylene biosynthesis by the aminotransferase VAS1. *Nat. Chem. Biol.* **2013**, *9*, 244–246. [CrossRef] [PubMed]
23. Zhao, Y.; Christensen, S.K.; Fankhauser, C.; Cashman, J.R.; Cohen, J.D.; Weigel, D.; Chory, J. A Role for Flavin Monooxygenase-Like Enzymes in Auxin Biosynthesis. *Science* **2001**, *291*, 306–309. [CrossRef] [PubMed]
24. Zazímalová, E.; Murphy, A.S.; Yang, H.; Hoyerová, K.; Hosek, P. Auxin transporters—Why so many? *Cold Spring Harb. Perspect. Biol.* **2010**, *2*, a001552. [CrossRef] [PubMed]
25. Barbez, E.; Kubeš, M.; Rolčík, J.; Béziat, C.; Pěnčík, A.; Wang, B.; Rosquete, M.R.; Zhu, J.; Dobrev, P.I.; Lee, Y.; et al. A novel putative auxin carrier family regulates intracellular auxin homeostasis in plants. *Nature* **2012**, *485*, 119–122. [CrossRef]
26. Fukaki, H.; Tasaka, M. Hormone interactions during lateral root formation. *Plant Mol. Biol.* **2008**, *69*, 437–449. [CrossRef]
27. Blilou, I.; Xu, J.; Wildwater, M.; Willemsen, V.; Paponov, I.; Friml, J.; Heidstra, R.; Aida, M.; Palme, K.; Scheres, B. The PIN auxin efflux facilitator network controls growth and patterning in *Arabidopsis* roots. *Nature* **2005**, *433*, 39–44. [CrossRef]
28. Gälweiler, L.; Guan, C.; Müller, A.; Wisman, E.; Mendgen, K.; Yephremov, A.; Palme, K. Regulation of Polar Auxin Transport by AtPIN1 in *Arabidopsis* Vascular Tissue. *Science* **1998**, *282*, 2226–2230. [CrossRef]
29. Friml, J.; Vieten, A.; Sauer, M.; Weijers, D.; Schwarz, H.; Hamann, T.; Offringa, R.; Jürgens, G. Efflux-dependent auxin gradients establish the apical–basal axis of Arabidopsis. *Nature* **2003**, *426*, 147–153. [CrossRef]
30. Blakeslee, J.J.; Bandyopadhyay, A.; Lee, O.R.; Mravec, J.; Titapiwatanakun, B.; Sauer, M.; Makam, S.N.; Cheng, Y.; Bouchard, R.; Adamec, J.; et al. Interactions among PIN-FORMED and P-Glycoprotein Auxin Transporters in *Arabidopsis*. *Plant Cell* **2007**, *19*, 131–147. [CrossRef]
31. Chen, Q.; Liu, Y.; Maere, S.; Lee, E.; Van Isterdael, G.; Xie, Z.; Xuan, W.; Lucas, J.; Vassileva, V.; Kitakura, S.; et al. A coherent transcriptional feed-forward motif model for mediating auxin-sensitive PIN3 expression during lateral root development. *Nat. Commun.* **2015**, *6*, 8821. [CrossRef]
32. Rakusová, H.; Abbas, M.; Han, H.; Song, S.; Robert, H.S.; Friml, J. Termination of Shoot Gravitropic Responses by Auxin Feedback on PIN3 Polarity. *Curr. Biol.* **2016**, *26*, 3026–3032. [CrossRef]
33. Žádníková, P.; Petrášek, J.; Marhavý, P.; Raz, V.; Vandenbussche, F.; Ding, Z.; Schwarzerová, K.; Morita, M.T.; Tasaka, M.; Hejátko, J.; et al. Role of PIN-mediated auxin efflux in apical hook development of *Arabidopsis thaliana*. *Development* **2010**, *137*, 607–617. [CrossRef]
34. Willige, B.C.; Chory, J. A current perspective on the role of AGCVIII kinases in PIN-mediated apical hook development. *Front. Plant Sci.* **2015**, *6*, 767. [CrossRef]
35. Hu, S.; Liu, X.; Xuan, W.; Mei, H.; Li, J.; Chen, X.; Zhao, Z.; Zhao, Y.; Jeyaraj, A.; Periakaruppan, R.; et al. Genome-wide identification and characterization of PIN-FORMED (PIN) and PIN-LIKES (PILS) gene family reveals their role in adventitious root development in tea nodal cutting (*Camellia sinensis*). *Int. J. Biol. Macromol.* **2023**, *229*, 791–802. [CrossRef]
36. Wang, W.; Gu, L.; Ye, S.; Zhang, H.; Cai, C.; Xiang, M.; Gao, Y.; Wang, Q.; Lin, C.; Zhu, Q. Genome-wide analysis and transcriptomic profiling of the auxin biosynthesis, transport and signaling family genes in moso bamboo (*Phyllostachys heterocycla*). *BMC Genom.* **2017**, *18*, 870. [CrossRef]
37. Feraru, E.; Feraru, M.I.; Barbez, E.; Waidmann, S.; Sun, L.; Gaidora, A.; Kleine-Vehn, J. PILS6 is a temperature-sensitive regulator of nuclear auxin input and organ growth in *Arabidopsis thaliana*. *Proc. Natl. Acad. Sci. USA* **2019**, *116*, 3893–3898. [CrossRef]
38. Goldental-Cohen, S.; Israeli, A.; Ori, N.; Yasuor, H. Auxin Response Dynamics During Wild-Type and entire Flower Development in Tomato. *Plant Cell Physiol.* **2017**, *58*, 1661–1672. [CrossRef]
39. Guilfoyle, T.J.; Hagen, G. Auxin response factors. *Curr. Opin. Plant Biol.* **2007**, *10*, 453–460. [CrossRef]
40. Abel, S.; Nguyen, M.D.; Theologis, A. The PS-IAA4/5-like family of early auxin-inducible mRNAs in *Arabidopsis thaliana*. *J. Mol. Biol.* **1995**, *251*, 533–549. [CrossRef]

41. Rouse, D.; Mackay, P.; Stirnberg, P.; Estelle, M.; Leyser, O. Changes in Auxin Response from Mutations in an *AUX/IAA* Gene. *Science* **1998**, *279*, 1371–1373. [CrossRef] [PubMed]
42. Leyser, H.O.; Pickett, F.B.; Dharmasiri, S.; Estelle, M. Mutations in the AXR3 gene of Arabidopsis result in altered auxin response including ectopic expression from the SAUR-AC1 promoter. *Plant J.* **1996**, *10*, 403–413. [CrossRef] [PubMed]
43. Deng, Y.; Chen, K.; Teng, W.; Zhan, A.; Tong, Y.; Feng, G.; Cui, Z.; Zhang, F.; Chen, X. Is the inherent potential of maize roots efficient for soil phosphorus acquisition? *PLoS ONE* **2014**, *9*, e90287. [CrossRef] [PubMed]
44. Luo, L.; Wan, Q.; Yu, Z.; Zhang, K.; Zhang, X.; Zhu, S.; Wan, Y.; Ding, Z.; Liu, F. Genome-Wide Identification of Auxin Response Factors in Peanut (*Arachis hypogaea* L.) and Functional Analysis in Root Morphology. *Int. J. Mol. Sci.* **2022**, *23*, 5309. [CrossRef]
45. Markakis, M.N.; Boron, A.K.; Van Loock, B.; Saini, K.; Cirera, S.; Verbelen, J.-P.; Vissenberg, K. Characterization of a Small Auxin-Up RNA (SAUR)-Like Gene Involved in *Arabidopsis thaliana* Development. *PLoS ONE* **2013**, *8*, e82596. [CrossRef]
46. Liu, S.; Xuan, L.; Xu, L.-A.; Huang, M.; Xu, M. Molecular cloning, expression analysis and subcellular localization of four DELLA genes from hybrid poplar. *Springerplus* **2016**, *5*, 1129. [CrossRef]
47. Li, Y.; Wang, Y.; Tan, S.; Li, Z.; Yuan, Z.; Glanc, M.; Domjan, D.; Wang, K.; Xuan, W.; Guo, Y.; et al. Root Growth Adaptation is Mediated by PYLs ABA Receptor-PP2A Protein Phosphatase Complex. *Adv. Sci.* **2020**, *7*, 1901455. [CrossRef]
48. Gonzalez-Rizzo, S.; Crespi, M.; Frugier, F. The *Medicago truncatula* CRE1 Cytokinin Receptor Regulates Lateral Root Development and Early Symbiotic Interaction with *Sinorhizobium meliloti*. *Plant Cell* **2006**, *18*, 2680–2693. [CrossRef]
49. Ramírez-Carvajal, G.A.; Morse, A.M.; Dervinis, C.; Davis, J.M. The Cytokinin Type-B Response Regulator PtRR13 Is a Negative Regulator of Adventitious Root Development in *Populus*. *Plant Physiol.* **2009**, *150*, 759–771. [CrossRef]
50. Xie, L.; Chen, F.; Du, H.; Zhang, X.; Wang, X.; Yao, G.; Xu, B. Graphene oxide and indole-3-acetic acid cotreatment regulates the root growth of *Brassica napus* L. via multiple phytohormone pathways. *BMC Plant Biol.* **2020**, *20*, 101. [CrossRef]
51. Deng, Y.; Wang, C.; Zhang, M.; Wei, L.; Liao, W. Identification of Key Genes during Ethylene-Induced Adventitious Root Development in Cucumber (*Cucumis sativus* L.). *Int. J. Mol. Sci.* **2022**, *23*, 12981. [CrossRef]
52. Zhu, J.Y.; Sae-Seaw, J.; Wang, Z.Y. Brassinosteroid signalling. *Development* **2013**, *140*, 1615–1620. [CrossRef]
53. Hacham, Y.; Holland, N.; Butterfield, C.; Ubeda-Tomas, S.; Bennett, M.J.; Chory, J.; Savaldi-Goldstein, S. Brassinosteroid perception in the epidermis controls root meristem size. *Development* **2011**, *138*, 839–848. [CrossRef]
54. Oblessuc, P.R.; Obulareddy, N.; DeMott, L.; Matiolli, C.C.; Thompson, B.K.; Melotto, M. JAZ4 is involved in plant defense, growth, and development in *Arabidopsis*. *Plant J.* **2020**, *101*, 371–383. [CrossRef]
55. Ranjan, A.; Perrone, I.; Alallaq, S.; Singh, R.; Rigal, A.; Brunoni, F.; Chitarra, W.; Guinet, F.; Kohler, A.; Martin, F.; et al. Molecular basis of differential adventitious rooting competence in poplar genotypes. *J. Exp. Bot.* **2022**, *73*, 4046–4064. [CrossRef]
56. Lakehal, A.; Chaabouni, S.; Cavel, E.; Le Hir, R.; Ranjan, A.; Raneshan, Z.; Novák, O.; Păcurar, D.I.; Perrone, I.; Jobert, F.; et al. A Molecular Framework for the Control of Adventitious Rooting by TIR1/AFB2-Aux/IAA-Dependent Auxin Signaling in *Arabidopsis*. *Mol. Plant.* **2019**, *12*, 1499–1514. [CrossRef]
57. Lakehal, A.; Dob, A.; Rahneshan, Z.; Novák, O.; Escamez, S.; Alallaq, S.; Strnad, M.; Tuominen, H.; Bellini, C. *ETHYLENE RESPONSE FACTOR 115* integrates jasmonate and cytokinin signaling machineries to repress adventitious rooting in *Arabidopsis*. *New Phytol.* **2020**, *228*, 1611–1626. [CrossRef]